The National Science Foundation's Daniel K. Inouye Solar Telescope

Thomas Rimmele and the DKIST Team
National Solar Observatory

ABSTRACT

The National Science Foundation's 4m Daniel K. Inouye Solar Telescope (DKIST) on Haleakala, Maui is now the largest solar telescope in the world. DKIST's superb resolution and polarimetric sensitivity will enable astronomers to unravel many of the mysteries the Sun presents, including the origin of solar magnetism, the mechanisms of coronal heating and drivers of flares and coronal mass ejections. Five instruments, four of which provide highly sensitive measurements of solar magnetic fields, including the illusive magnetic field of the faint solar corona. The design allows DKIST to operate as a coronagraph at infrared wavelengths where the sky background is low and bright coronal emission lines are available. The high-order, single-conjugate adaptive optics system (AO) provides diffraction limited imaging and the ability to resolve features approximately 20 km on the Sun. A multi-conjugate AO upgrade is in progress. Achieving this resolution is critical for the ability to observe magnetic structures at their fundamental scales. With these unique capabilities DKIST will address basic research aspects of Space Weather and help improve predictive capabilities. The DKIST instruments will produce large and complex data sets, which will be distributed through the NSO/DKIST Data Center. DKIST has achieved first engineering solar light in December of 2019. Due to COVID the start of the operations commissioning phase is delayed and is now expected for fall of 2021. This paper discusses science objectives, DKIST design, and presents first images and movies obtained with DKIST.

1. INTRODUCTION

The US National Science Foundation's (NSF) 4 m DKIST on Haleakalā, Maui, Hawai'i is the largest solar telescope in the world. A detailed description of the design and capabilities of the DKIST observatory, as well as a comprehensive list of references are provided by [1]. DKIST delivers spatial resolution and sensitivity that enable astronomers to unravel many of the mysteries the Sun presents, including the origin of solar magnetism, the mechanisms of coronal heating and drivers of the solar wind, flares, coronal mass ejections, and variability in solar output. The adaptive-optics system provides diffraction-limited imaging and the ability to resolve features approximately 20 km on the Sun. Resolving spatial scales on the order of a few tens of kilometers is of crucial importance to be able to test physical models and thus understand how the physics of the small scales ties into the larger-scale problems.

Measurements of the solar magnetic field of sufficient resolution and sensitivity and throughout the solar atmosphere, including the corona, are key to solving many of the outstanding problems of solar astronomy. The DKIST critical science plan compiles a large number of science use cases, i.e., observation, that will be carried out in the early years of DKIST operations [2]. Five instruments, four of which are polarimeters, will provide highly sensitive measurements of the solar magnetic field and other physical plasma parameters. The design allows DKIST to operate as a coronagraph at infrared wavelengths. Mapping of the coronal magnetic field is a key mission of DKIST, which was designed to address basic research aspects of space weather and help improve predictive capabilities. During its nominal lifetime of two magnetic solar cycles DKIST will provide observational data that will allow scientists to advance and refine models and simulations of solar phenomena.

The scientific mission of DKIST is relevant far beyond solar astronomy. Magnetic fields are ubiquitous throughout the universe and play a key role in, for example, early universe galaxy formation. Due to its proximity, the Sun provides us with a laboratory where fundamental physical processes that operate throughout the universe can be studied in detail that no other astronomical object affords us. The advances in our understanding of basic physical processes that DKIST provides will inform and help advance astronomy and other related fields, such as plasma physics.

Site construction of DKIST began in December 2012. First solar light was achieved in December 2019. Integration and commissioning of first-light instruments and instrument supporting systems is progressing through 2021. The COVID

pandemic resulted in a delay of the integration, test and instrument commissioning phase. The start of operations is now projected for mid-November, 2021. DKIST science operations are entirely driven by community proposals solicited through a regular proposal cycle. The first proposal call for the operations commissioning phase was released in May 2020. Observations and data collection for successful proposals will begin at the end of November, 2021.

2. OVERVIEW

Fig. 1 shows a rendering of the DKIST facility and its main subsystems. The main telescope is a 4 m off-axis Gregorian design. The optics is supported by the alt–az telescope mount structure, and is protected from the environment by a thermally controlled and well-ventilated enclosure. A number of optical elements relay the light beam to the environmentally controlled coudé lab where the suite of first-light instruments is located. The instruments are installed on a rotating platform, which serves as image de-rotator and allows alignment of the spectrograph slits. The tip-tilt mirror and the deformable mirror of the conventional high order AO system are integrated into the transfer optics. The AO corrected light beam feeds the four instruments that are designed to perform diffraction-limited observations at visible- and near-infrared wavelengths. Facility buildings include a support-and-operations building. The utility building is to the side of the main observatory and houses mechanical equipment, such as chillers, pumps, air-handling units, and electrical equipment. Fig. 2 displays an image of the completed DKIST at the Haleakalā Observatory site.

The DKIST Science Support Center (DSSC) in Pukalani serves as the DKIST base facility and provides office and lab space. Operations assistance and eventually remote operations can be performed from the DSSC.

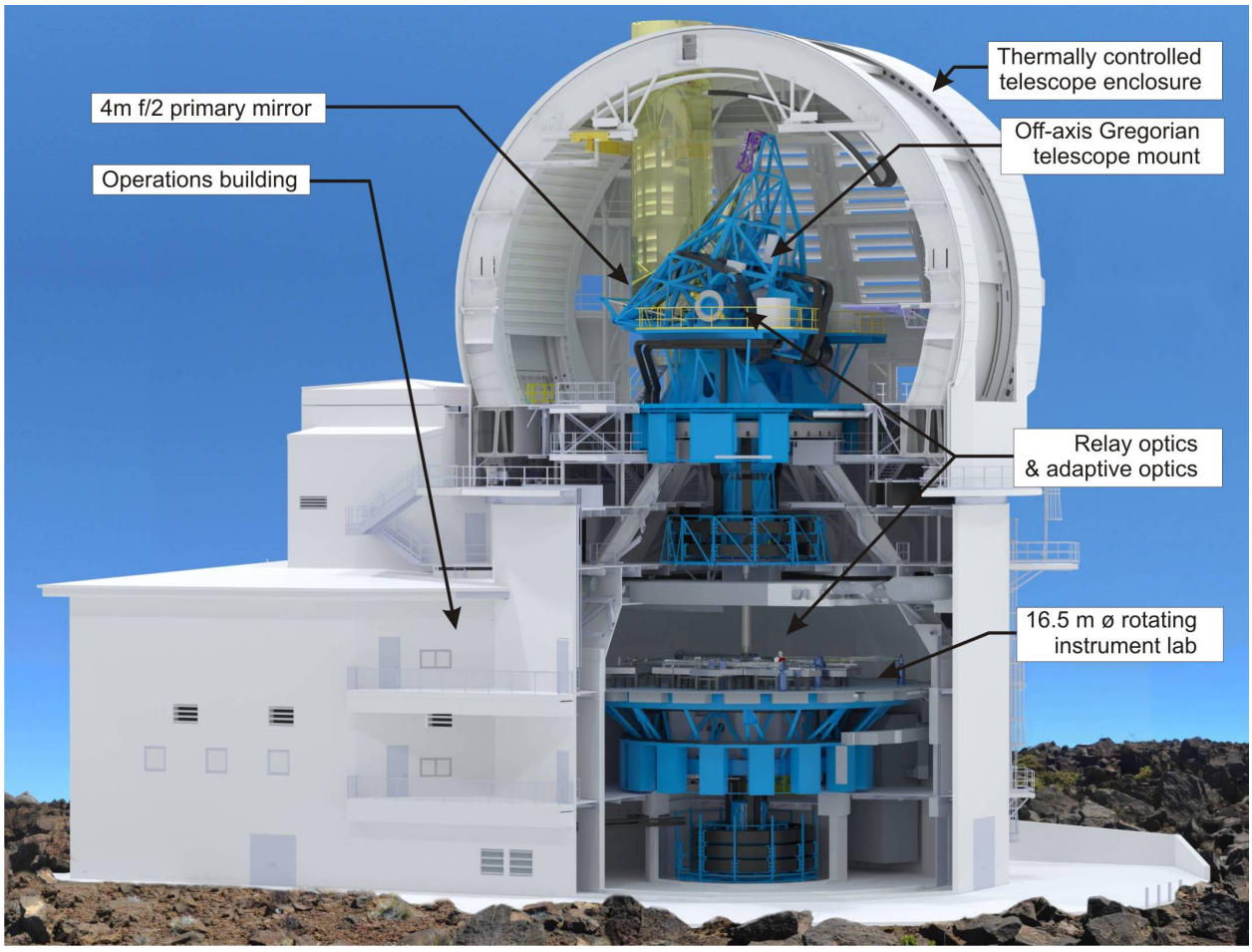

Fig. 1: Schematic of DKIST facility and its major components. The overall facility height is 41.4 m. The diameter of the rotating instrument platform is 16.5 m.

Fig. 2: The outside of the completed DKIST on Haleakalā. The telescope building with lower, and upper enclosure and the attached Support and Operations building, including platform lift used to transport M1 to the telescope level, are shown on the right of the image. Vent gates ensure sufficient air flow through the enclosure during operations. The utility building, which supplies coolant to the main facility and houses backup power systems is visible to the right of the main facility. The overall facility height is 41.4 m

2.1 Telescope Design

DKIST is designed as an unobstructed, off-axis Gregorian telescope. The alt–az telescope mount provides for slewing, pointing, and tracking throughout altitude and azimuth rotations. Major optics groups include:

i) The main telescope consisting of primary and secondary mirrors, a heat-stop and a Lyot-stop. Integrated into the main telescope is the Gregorian Optical Station (GOS), which houses calibration systems.

ii) The transfer optics, direct the light along elevation and azimuth axis of the telescope mount and down to the coudé lab.

iii) The coudé optics, which provide a collimated beam and an image of the entrance aperture for the DM.

iv) The facility instrument-distribution optics (FIDO), which in a reconfigurable manner distribute light to the various instruments.

Fig. 3 shows the off-axis Gregorian telescope and the alt-az mount. The telescope is located with the co-rotating enclosure. The active support of the primary is apparent in this image.

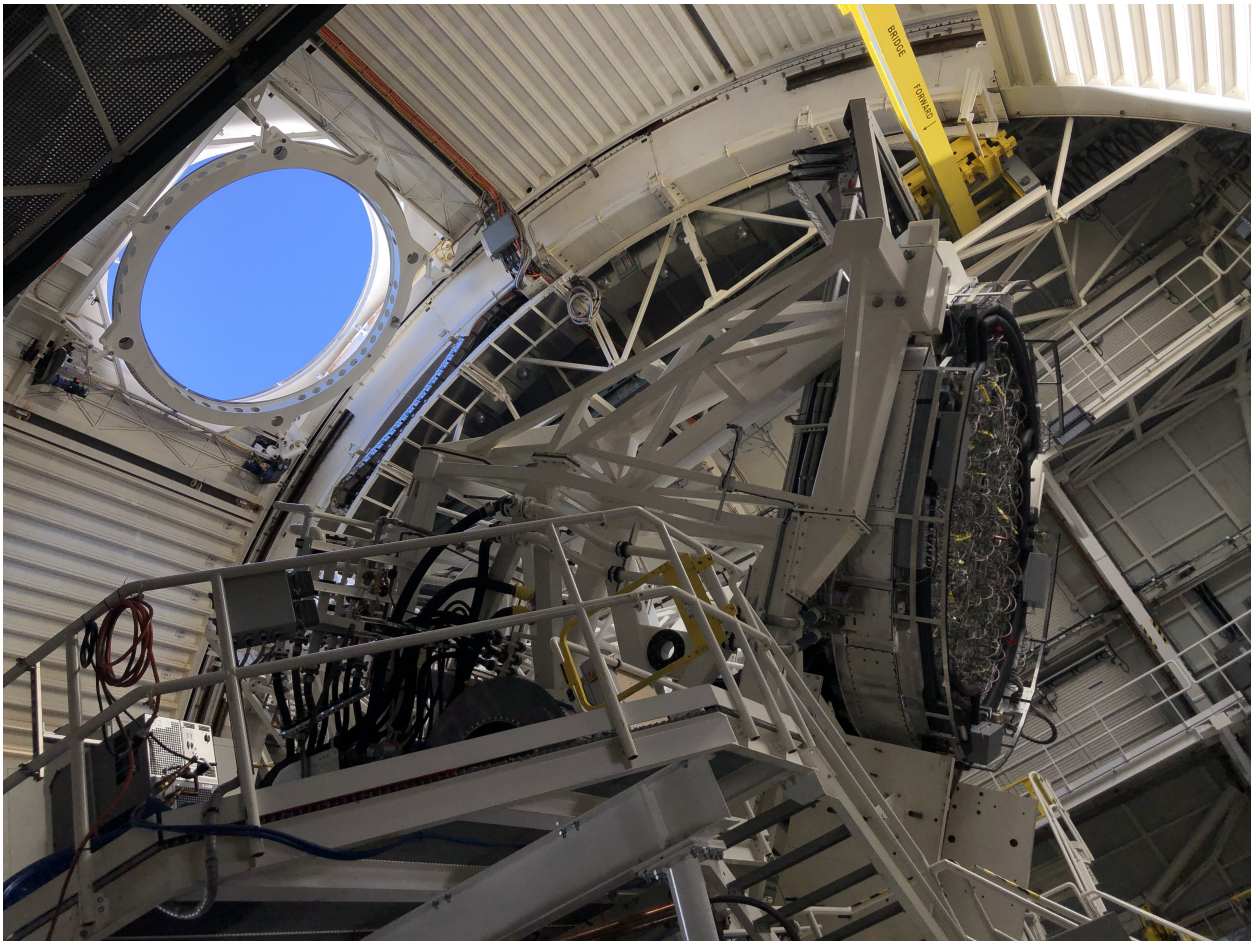

Fig. 3: Off-axis Gregorian telescope and alt-az mount of DKIST.

The primary (M1) is a 4 m off-axis,f/2 parabola. The secondary mirror is a 0.65 m concave ellipsoid (conic constant = -0.54. A heat stop at prime focus passes a 5 arcmin science FOV and rejects most of the 13 kW solar heat load. The scientific and technical drivers for the off-axis design include: a) The unobstructed aperture provides the full 12.56 m^2 collecting area and is free from the diffraction effects of the secondary mirror and its support spider, which would

negatively impact the coronal science objectives. b) The off-axis location of the secondary mirror provides physical space to implement the heat stop at prime focus and the required cooling lines. The secondary mirror can also be sheltered from wind buffeting and supported in a more robust way than is possible in an on-axis configuration. M1 is coated with unprotected aluminum at the coating facility located on Haleakalā at the Air Force Maui Optical Station (AMOS). All other mirrors are coated with protected silver in order to achieve high transmission of the optical system.

Fig. 4: The DKIST Science Support Center (DSSC) in Pukalani, Maui, Hawai'i. This base facility provides office and lab space and includes a remote operations room from which observations can be monitored and guided by science staff.

M1 is a 75 mm thin meniscus is made form Zerodur and is actively supported by 118 axial actuators and 24 lateral supports. In order to avoid mirror seeing the front surface of M1 is maintained at close to ambient temperatures using air-jet cooling from the backside of the mirror. To minimize scattered light from dust contamination, special equipment was designed and built to allow for frequent CO_2 cleaning and in-situ washing. M2 is made of a light-weight SiC structure and serves as fast steering mirror. A thermal control system maintains the front surface temperature of M2 within $\pm$ 1 ^{o}C of ambient via air jet impingement on its back surface. The off-axis M2 produces an f/13 beam that provides a secondary image at the Gregorian Optical Station (GOS). The f/2 M1 forms an image of the solar disk in prime focus where the reflecting heat-stop is located. The image size is approximately 75 mm. The heat-load at prime focus is approximately 2.5 MW/m^2. The mount supporting the off-axis telescope optics gives the appearance of being unbalanced. However, large counterweights are used to balance the system and enable very accurate pointing and tracking.

DKIST instruments are mounted on a large coudé-rotator platform. The coudé rotator platform is 16.5 meters in diameter and weighs approximately 115 tons. Given its size, mass, and its critical function of maintaining a precise and stable optical path to the instrument detectors, the coudé rotator has exacting requirements on its motion and deviations from that motion (deflection and jitter) as it tracks a target. For example, a lateral bearing run-out of approximately 50 micron has been achieved for this massive structure.

2.2 Active and Adaptive Optics

The wavefront correction system is a key component of DKIST that enables both seeing-limited and diffraction-limited observations. This subsystem includes:

i) A solar AO system that corrects atmospheric seeing and residual optical aberrations at 2 kHz rates. The main

components of AO are the 1600-actuator Deformable Mirror (DM), and a fast tip-tilt mirror (M5). The wave front sensor is a correlating Shack–Hartmann sensor [3] with 1457 sub-apertures.

ii) An active optics (aO) system that corrects slowly changing aberrations that may arise primarily from gravitational and thermal deformations of the telescope structure. The aO system ensures that the M1 surface figure remains within allowed tolerances during operations by making adjustments to the active mount of M1. The hexapod-mounted M2 is also used as a corrector primarily for focus (z-motion).

iii) Active alignment. Wavefront sensors and LUT information are used to keep pupil images and boresight in alignment. M3 and M6 are used to correct small drifts that might occur, for example, while the coudé rotator spins around its axis.

The AO system is capable of correcting up to approximately 1400 Karhunen—Loève (KL) modes and achieves Strehl ratios of $S > 0.3$ for $r_0(500\,\mathrm{nm}) > 7\,\mathrm{cm}$ (close to median seeing) and $S > 0.6$ for $r_0(630\,\mathrm{nm}) > 20\,\mathrm{cm}$.

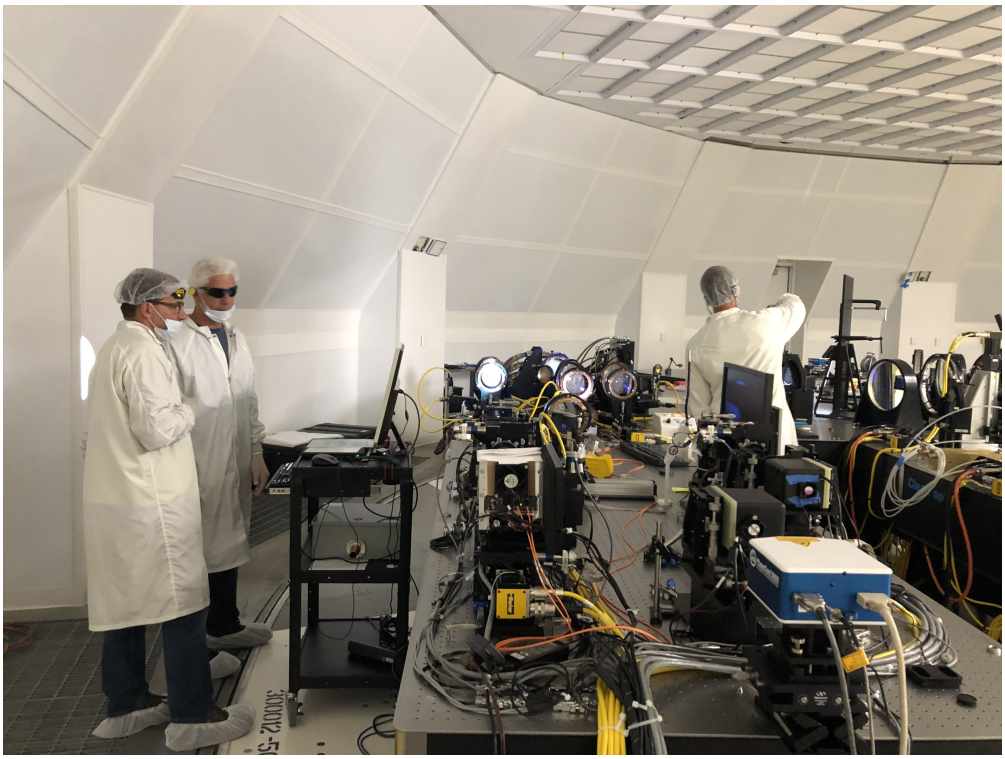

Fig. 5: Wavefront-correction bench during first solar light achieved at the coudé instrument lab.

M1 figure control and alignment functions can be performed with previously established LUTs or using wavefront sensor outputs from either the AO or aO, respectively, depending on the operational mode. Both the aO wavefront sensor and AO wavefront sensors provide time-averaged wavefront measurements. By averaging over the atmospheric seeing, information about slowly varying aberrations due to optical misalignment and/or M1 figure deformations is provided to the wavefront control system. The system architecture and the optical design of the wavefront sensors and context viewer were described in much detail in [4]. Integration and system testing are summarized by [5]. The Field-Programmable-Gate-Array (FPGA) based real-time control of the AO and its integration into the overall active- and adaptive-wavefront control concept are described by [6].

First on-sky data with the wavefront-correction system in operation were obtained during the first-light initiative in December, 2019. The high- and low-order wavefront sensors and the context viewer, which produced the sunspot image shown in Section 5, are displayed with this image. The AO system delivered Strehl ratios as estimated from

wavefront-sensor telemetry very close to specifications [5], enabling the diffraction-limited first-light imaging presented in Section 5.

Fig. 6: DKIST instrument laboratory. The coude instrument lab provides a temperature controlled clean-room environment. Instruments and feed-optics are mounted on the coude rotator platform. The locations of the individual instruments are pointed out with arrows. The VTF is a partner contribution from Germany and arrives in 2022.

Although not part of the construction-project scope, an upgrade from conventional AO to MCAO [7] was envisioned early on in the project. The optical design can accommodate additional DMs at conjugates of turbulence layers in the upper atmosphere. M7 and M9 are conjugate to 11 km and 4 km height in the Earth's atmosphere, respectively, and thus in near-optimal location for a three DM MCAO system. Design and prototyping of the MCAO upgrade are ongoing.

sectionThermal Systems Minimization of seeing effects was a major design consideration. The infrastructure implemented to provide the thermal control and thus internal-seeing mitigation strategies is substantial and complex. Optical surfaces and a number of structural elements are controlled to ambient temperatures to avoid local seeing effects that would negatively impact the AO performance. For example, sections of the dome skin are actively cooled. The coudé lab is temperature stabilized to $20 \pm 0.5\,^{o}$C , which ensures stability of instruments and their calibrations. An air-knife separates the environmentally controlled coudé lab from the enclosure environment. The air knife is installed along the optical path between M6 and M7 and provides a strong, laminar cross flow. While the coudé lab is maintained to 0.5 ^{o}C at 20 ^{o}C, the inside of the enclosure experiences large swings as the outside temperature changes during the day and during the year. To avoid absorption of IR wavelengths, a glass window can not be used to separate the two environments. The laminar cross-flow prevents turbulence at the interface where a large temperature differential might exist.

During day-time operations, cooling capacity is provided by the ice storage tanks. Approximately 12 kilometers of pipes distribute coolant throughout the facility. Three large air handling units are part of the thermal control system. A sophisticated control system provides master control to the distributed elements in order to safely and economically monitor and operate the thermal equipment and control site power demand.

3. POLARIMETRY

Many observing use-cases call for simultaneous observations of multiple wavelengths spanning ultraviolet to infrared wavelengths. Instruments have a wide range of polarimetric sensitivity and accuracy requirements. The DKIST project has undertaken a large system-level effort to understand the polarization performance and limiting errors covering this very wide range of scenarios. A common way of summarizing polarization errors in an optical system, which includes the telescope, relay optics, FIDO dichroics, instrument feed optics, and the instruments, is to describe how errors in various sub-matrices within the system Mueller matrix impact the accuracy of the reconstructed Stokes vector for the solar beam. DKIST has expended substantial effort towards understanding and minimizing polarization-error sources. These efforts have given DKIST a detailed system-level knowledge of the optical performance. Thorough testing of instrument-level alignment stability and camera-sensor performance provide an understanding of errors within each facility instrument. An inter-disciplinary set of new modeling mathematics and algorithms coupled with

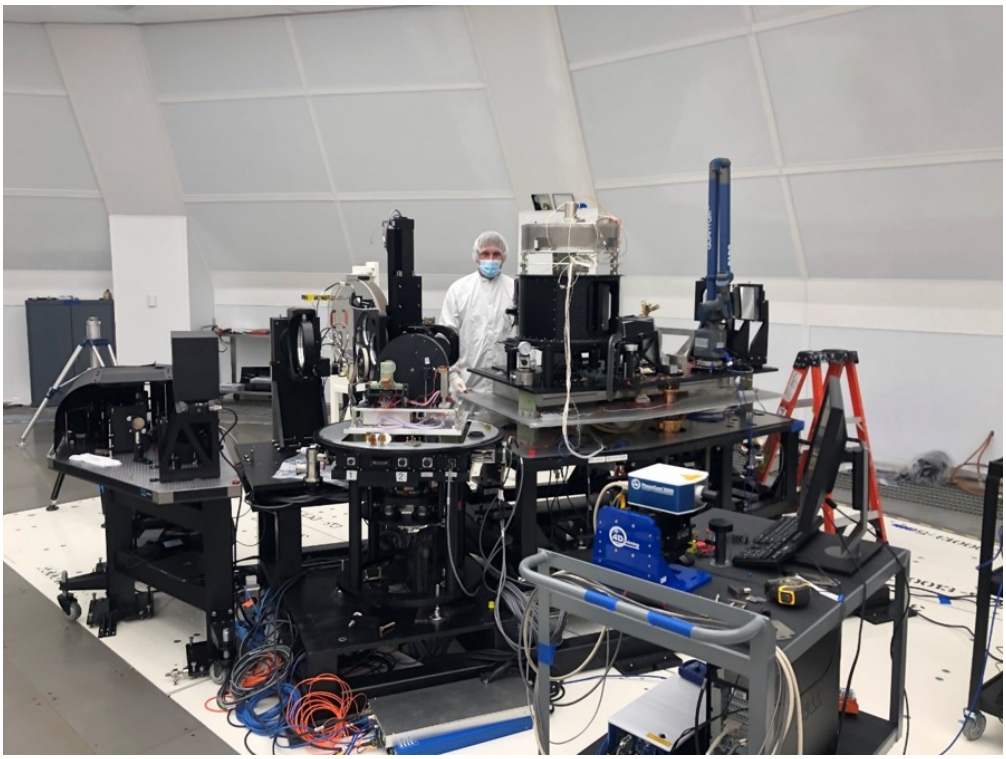

Fig. 7: CRYO NIRSP. As an example for size and complexity of DKIST instruments the CRYO NIRSP, which was built at the UH/IfA on Maui, is shown.

new laboratory tools for detailed characterization of optical elements was developed. Mueller-matrix spatial–spectral mapping systems covering UV to IR wavelengths were developed and utilized to characterize optics [8]. Retarders were spatially mapped, characterized for elliptical retardance, and this ellipticity is included in the calibration process. The mirror-coating polarization was measured for every coated surface in the system including all instrument optics and facility dichroics [9]. A dual fiber-fed spectrograph system was designed and deployed to calibrate DKIST, including the CRYO-NIRSP feed optics and covering 390 nm to 165 nm, which represents the majority of the proposed science use cases for early operations. Preliminary system model calibrations were successful [10]. The suite of facility dichroics that feed the AO-assisted instruments have open-source coating designs have been characterized for their polarization performance in both reflection and transmission and also for spatial uniformity of coating-polarization properties.

4. INSTRUMENTATION

The initial set of facility instrumentation includes the Visible Broad-band Imager (VBI: [11]), the Visible Spectro-Polarimeter (ViSP: [12]), the Diffraction-Limited Near-Infrared Spectro-Polarimeter (DL-NIRSP: [13]), the Cryogenic Near-Infrared Spectro-Polarimeter (CRYO-NIRSP: [14]), and the Visible Tunable Filter (VTF: [15]). All instruments, except for the CRYO-NIRSP, are provided with an AO-corrected beam.

4.1 Visual Broadband Imager

The VBI [11] is designed to provide diffraction-limited images and movies at a number of wavelengths that image the photosphere and the chromospheres. A filter that enables high-resolution imaging of coronal structures is also included. The VBI and its science mission, and capabilities are described in previous publications [16]. The instrument is divided into a red and a blue channel. In combination the two channels cover the wavelengths range 390 nm to 860 nm. The CMOS cameras provide a 4k×4k image stream at a frame rate of up to 30 Hz. The VBI achieves the full resolution potential of the 4 m DKIST by using AO and quasi-real-time speckle image reconstruction at a three-second cadence.

4.2 Visible Spectro-Polarimeter

The ViSP provides precision measurements of the full state of polarization (i.e. all four Stokes parameters I, Q, U, and V) simultaneously at diverse wavelengths in the visible spectrum, while fully resolving the spectral profiles of spectrum lines originating in the solar atmosphere. Such measurements provide quantitative diagnostics of the magnetic field vector as a function of height in the solar atmosphere, along with the associated variation of the thermodynamic properties. Wavelength diversity is a key element of the instrument allowing the ViSP to simultaneously perform spectro-polarimetric maps in up to three arbitrarily chosen and widely separated lines in the visible and near-infrared spectral range (380 nm – 900 nm). The High Altitude Observatory in Boulder, Colorado has been leading the design and implementation of the ViSP ([12]).

4.3 Visible Tunable Filter

The VTF enables rapid imaging spectroscopy and polarimetry. The dual-etalon Fabry–Perot filter covers the wavelength range from 515 nm to 860 nm. The spectral resolution of the Fabry–Perot (FP) filter system is 6 pm at 600 nm. The FOV is limited by the physical size of the FP to 1 arcmin. The 4k×4k pixel detectors enables Nyquist sampling at visible wavelengths providing a spatial resolution of 0.028 arcsec on the sky (20 km on the Sun). A full Stokes-vector measurement in two spatial dimensions and with a polarimetric sensitivity of 5×10^{-3} can be recorded within 13 seconds. The VTF uses three detectors: two for the polarimetric measurements, and one for broadband filtergrams. The science goals and main scientific observables, instrument requirements, design, and performance modeling were described by [17] and [18]. The VTF design and construction is being led by the Leibniz Institute in Freiburg, Germany as a partnership contribution to the DKIST. The instrument is currently undergoing lab integration.

4.4 Diffraction-Limited Near-Infrared Spectro-Polarimeter

The DL-NIRSP [13] is an integral-field, dual-beam spectro-polarimeter intended for studying magnetically sensitive spectral lines in the Sun's atmosphere with high spectral resolution (125,000) and polarimetric accuracy. A novel fiber-optic integral field unit, paired with selectable feed optics and a field-scanning mirror provide different spatial sampling (0.03 arcsec, 0.08 arcsec, and 0.5 arcsec). Multiple wavelengths can be observed simultaneously using three spectral arms to cover visible (500 – 900 nm) and infrared wavelengths (900 – 1350 nm and 1350 – 1800 nm). DL-NIRSP's science mission includes measurements of the coronal magnetic field when DKIST. The instrument was designed and built by the University of Hawai'i's Institute for Astronomy (IfA).

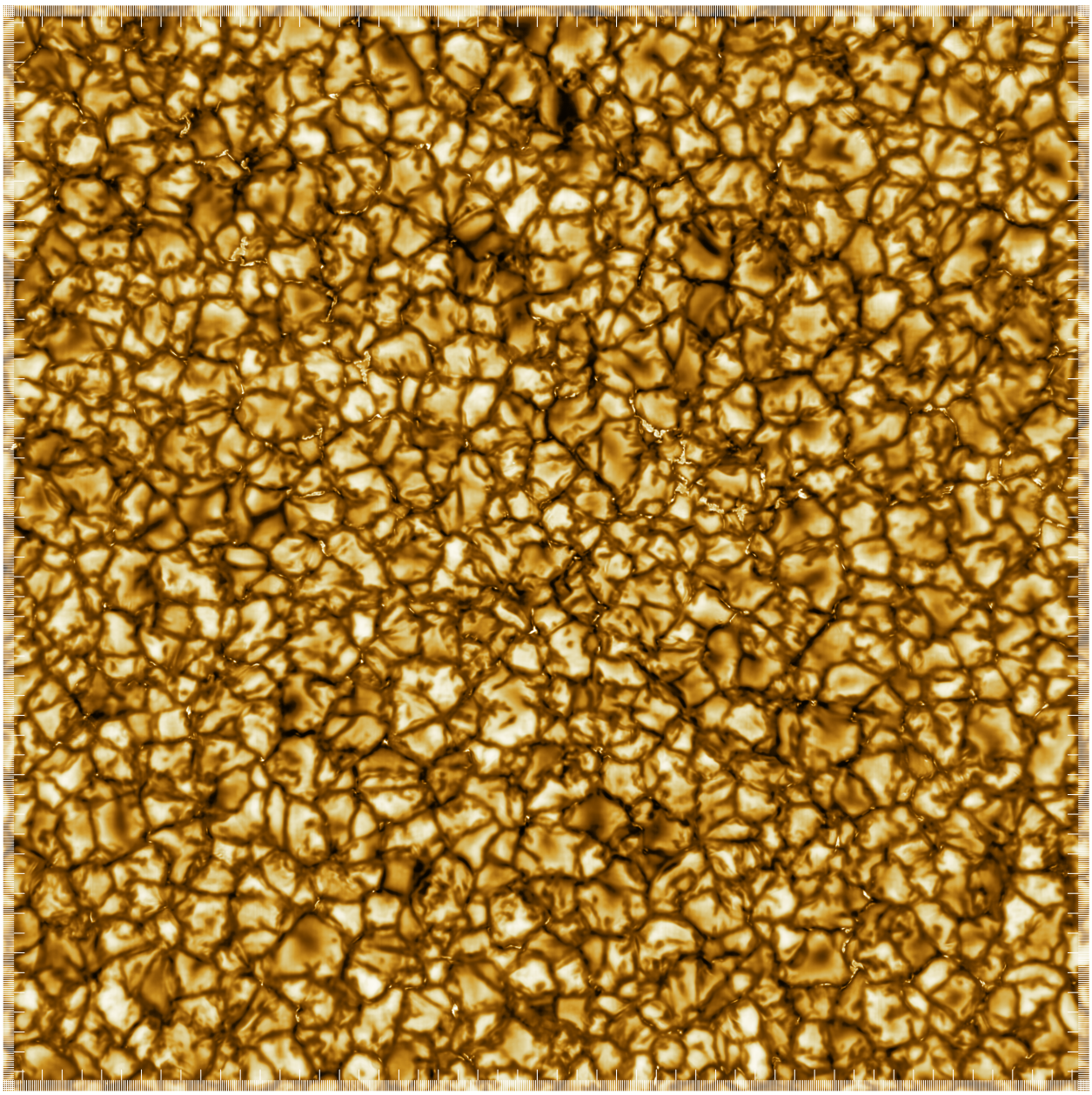

Fig. 8: First light image of granulation near Sun-center taken with VBI red. The FOV is 55 arcsec$\times$55 arcsec (major tick marks are 1 arcsec). A burst of 80 short exposure images was speckle reconstructed. The resolution achieved with this image is close to the diffraction limit at the wavelength of 789 nm (0.04 arcsec). The Image was processed to remove noise and enhance the visibility (contrast) of small-scale (magnetic) features.

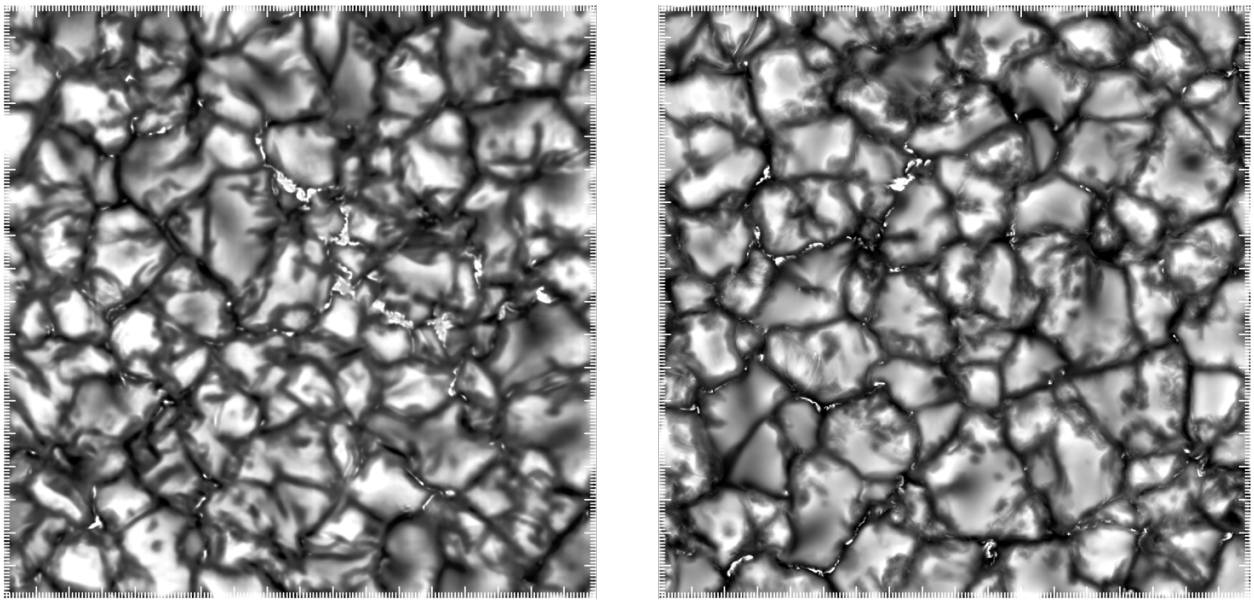

Fig. 9: Comparison DKIST observation (left) and MHD simulation (right, courtesy M. Rempel, HAO).

4.5 Cryogenic Near-Infrared Spectro-Polarimeter

The primary goal of the CRYO-NIRSP[14] is to measure the magnetic fields over a large FOV in the solar corona. The CRYO-NIRSP is designed to measure polarized light of coronal emission lines at infrared wavelength out to 5 microns. The CRYO-NIRSP has a large field of view (5 arcmin max) that can be sampled with a slit-scanning mechanism. By trading spatial and spectral resolution for enhanced signal-to-noise, coronal magnetic field measurements using spectral lines such as in Fe XIII (1075 nm) and Si IX (3935 nm) can be performed with sufficient sensitivity. Depending on the specific target, observations will be performed at a spatial resolution of 1 – 2 arcsec. Spectral resolution of up to R = 100000 is achieved. The spectrograph optics are cooled to cryogenic temperatures in order to reduce the thermal background allowing for mid-IR observations of the faint solar corona. CRYO-NIRSP provides the capability to perform on-disk observations at higher spatial resolution including at the important CO bands at 2333 nm and 4666 nm. The University of Hawai'i IfA, in partnership with NSO, has led the development of the CRYO-NIRSP.

The Data Handling System on the summit is used to collect, process, and display data from all instruments. All cameras transfer data to the DHS via multiple camera lines. The DHS transfers data from the various instrument cameras using a high-speed network to the large volume storage servers. The DHS provides quick-look displays and "sandbox processing" for more detailed quality control. The DHS on the summit is the interface to the DKIST Data Center in Boulder for all instruments.

5. FIRST LIGHT AND FIRST RESULTS

First images with DKIST were recorded in December 2019. The VBI red obtained bursts of granulation images using its 789 nm and 705 nm filters. The AO system was locked on granulation for the first time as well. VBI 4k×4k images were taken at a rate of 30 Hz. Bursts of 80 – 100 images were recorded with a cadence of three seconds. Several time sequences of speckle bursts of up to 10 minutes were obtained over a period of three days. Images were subjected to standard dark- and flat-field calibration. Bursts of 80 images each were used to derive speckle reconstructed images [19]. Noise filtering was applied to remove camera noise. The image, which was used for the first light press release in January 2020 and received broad coverage in the international press, is shown with Fig.8.

Fig. 9 shows a comparison of a MHD simulated (MURaM) granulation image and a close-up of the observed granulation image displayed in Fig. 8. This comparison demonstrates that with DKIST we now have resolution comparable to the resolution of highest-resolution MHD simulations. However, detailed and quantitative verification of model

predictions must yet be performed by, e.g., comparing modeled and observed physical parameters, such as velocities, magnetic-field strengths and directions, intensities, and their temporal evolution. The iterative process of verifying and improving models and model assumptions based on observations will occur over many years to come.

6. SUMMARY

After more than two decades, the 4 m DKIST has finally come to fruition. First imagery clearly shows the potential of DKIST and its set of state-of-the-art instruments to revolutionize solar astronomy. The DKIST design represents an excellent balance of various design drivers that allows the pursuit of the many pressing science drivers by providing the most capable solar telescope facility built to date. Many technical challenges had to be addressed and difficult trades had to be performed to achieve this goal. Operations of DKIST are ramping up with the one-year Operations Commissioning Phase expected to begin in November of 2021. The first proposal call was released. Community response was overwhelming. The DKIST data center will serve several petabytes per year of calibrated data to the world-wide user community. As the DKIST data base builds up over time, many novel science projects will emerge from the vast amount of available data. The scientific exploitation is just beginning and DKIST will significantly advance our knowledge of the Sun over the next several decades.

7. ACKNOWLEDGEMENTS

The research reported herein is based in part on data collected with the *Daniel K. Inouye Solar Telescope* (DKIST), a facility of the National Solar Observatory (NSO). NSO is managed by the Association of Universities for Research in Astronomy, Inc., and is funded by the National Science Foundation. Any opinions, findings and conclusions or recommendations expressed in this publication are those of the authors and do not necessarily reflect the views of the National Science Foundation or the Association of Universities for Research in Astronomy, Inc. DKIST is located on land of spiritual and cultural significance to Native Hawaiian people. The use of this important site to further scientific knowledge is done so with appreciation and respect.

[1] Thomas R. Rimmele, Mark Warner, Stephen L. Keil, Philip R. Goode, Michael Knölker, Jeffrey R. Kuhn, Robert R. Rosner, Joseph P. McMullin, Roberto Casini, Haosheng Lin, Friedrich Wöger, Oskar von der Lühe, Alexandra Tritschler, Alisdair Davey, Alfred de Wijn, David F. Elmore, André Fehlmann, David M. Harrington, Sarah A. Jaeggli, Mark P. Rast, Thomas A. Schad, Wolfgang Schmidt, Mihalis Mathioudakis, Donald L. Mickey, Tetsu Anan, Christian Beck, Heather K. Marshall, Paul F. Jeffers, Jacobus M. Oschmann, Andrew Beard, David C. Berst, Bruce A. Cowan, Simon C. Craig, Eric Cross, Bryan K. Cummings, Colleen Donnelly, Jean-Benoit de Vanssay, Arthur D. Eigenbrot, Andrew Ferayorni, Christopher Foster, Chriselle Ann Galapon, Christopher Gedrites, Kerry Gonzales, Bret D. Goodrich, Brian S. Gregory, Stephanie S. Guzman, Stephen Guzzo, Steve Hegwer, Robert P. Hubbard, John R. Hubbard, Erik M. Johansson, Luke C. Johnson, Chen Liang, Mary Liang, Isaac McQuillen, Christopher Mayer, Karl Newman, Brialyn Onodera, LeEllen Phelps, Myles M. Puentes, Christopher Richards, Lukas M. Rimmele, Predrag Sekulic, Stephan R. Shimko, Brett E. Simison, Brett Smith, Erik Starman, Stacey R. Sueoka, Richard T. Summers, Aimee Szabo, Louis Szabo, Stephen B. Wampler, Timothy R. Williams, and Charles White. The Daniel K. Inouye Solar Telescope - Observatory Overview. *Solar Phys.*, 295(12):172, December 2020.

[2] Mark P. Rast, Nazaret Bello González, Luis Bellot Rubio, Wenda Cao, Gianna Cauzzi, Edward Deluca, Bart de Pontieu, Lyndsay Fletcher, Sarah E. Gibson, Philip G. Judge, Yukio Katsukawa, Maria D. Kazachenko, Elena Khomenko, Enrico Landi, Valentín Martínez Pillet, Gordon J. D. Petrie, Jiong Qiu, Laurel A. Rachmeler, Matthias Rempel, Wolfgang Schmidt, Eamon Scullion, Xudong Sun, Brian T. Welsch, Vincenzo Andretta, Patrick Antolin, Thomas R. Ayres, K. S. Balasubramaniam, Istvan Ballai, Thomas E. Berger, Stephen J. Bradshaw, Ryan J. Campbell, Mats Carlsson, Roberto Casini, Rebecca Centeno, Steven R. Cranmer, Serena Criscuoli, Craig Deforest, Yuanyong Deng, Robertus Erdélyi, Viktor Fedun, Catherine E. Fischer, Sergio J. González Manrique, Michael Hahn, Louise Harra, Vasco M. J. Henriques, Neal E. Hurlburt, Sarah Jaeggli, Shahin Jafarzadeh, Rekha Jain, Stuart M. Jefferies, Peter H. Keys, Adam F. Kowalski, Christoph Kuckein, Jeffrey R. Kuhn, David Kuridze, Jiajia Liu, Wei Liu, Dana Longcope, Mihalis Mathioudakis, R. T. James McAteer, Scott W. McIntosh, David E. McKenzie, Mari Paz Miralles, Richard J. Morton, Karin Muglach, Chris J. Nelson, Navdeep K. Panesar, Susanna Parenti, Clare E. Parnell, Bala Poduval, Kevin P. Reardon, Jeffrey W. Reep, Thomas A. Schad,

Donald Schmit, Rahul Sharma, Hector Socas-Navarro, Abhishek K. Srivastava, Alphonse C. Sterling, Yoshinori Suematsu, Lucas A. Tarr, Sanjiv Tiwari, Alexandra Tritschler, Gary Verth, Angelos Vourlidas, Haimin Wang, Yi-Ming Wang, NSO and DKIST Project, DKIST Instrument Scientists, DKIST Science Working Group, and DKIST Critical Science Plan Community. Critical Science Plan for the Daniel K. Inouye Solar Telescope (DKIST). *Solar Phys.*, 296(4):70, April 2021.

[3] Thomas R. Rimmele and Jose Marino. Solar Adaptive Optics. *Liv. Rev. Solar Phys.*, 8(1):2, June 2011.

[4] Luke C. Johnson, Keith Cummings, Mark Drobilek, Erik Johansson, Jose Marino, Kit Richards, Thomas Rimmele, Predrag Sekulic, and Friedrich Wöger. Status of the DKIST system for solar adaptive optics. In *Proc. Soc. Photo-Opt. Instrum. Eng. (SPIE)*, volume CS-9909, page 99090Y, July 2016.

[5] Luke C. Johnson, Erik Johansson, Kit Richards, Friedrich Wöger, Jose Marino, and Thomas Rimmele. First light with adaptive optics: The performance of the DKIST high-order adaptive optics. In *Proc. Soc. Photo-Opt. Instrum. Eng. (SPIE)*, page in preparation, 2020.

[6] K. Richards, T. Rimmele, S. L. Hegwer, R. S. Upton, F. Woeger, J. Marino, S. Gregory, and B. Goodrich. The adaptive optics and wavefront correction systems for the Advanced Technology Solar Telescope. In *Proc. Soc. Photo-Opt. Instrum. Eng. (SPIE)*, volume CS-7736, page 773608, July 2010.

[7] Dirk Schmidt, Nicolas Gorceix, Philip R. Goode, Jose Marino, Thomas Rimmele, Thomas Berkefeld, Friedrich Wöger, Xianyu Zhang, François Rigaut, and Oskar von der Lühe. Clear widens the field for observations of the Sun with multi-conjugate adaptive optics. *Astron. Astrophys.*, 597:L8, January 2017.

[8] David M. Harrington, Sarah Jaeggli, Tom Schad, Amanda J. White, and Stacey R. Sueoka. Polarization modeling and predictions for Daniel K. Inouye Solar Telescope part 6: Fringe Mitigation with Polycarbonate Modulators and Optical Contact Calibration Retarders. *J. Astron. Tel., Instr., Syst.*, 6, 2020.

[9] David M. Harrington, Stacey R. Sueoka, and Amanda J. White. Polarization modeling and predictions for Daniel K. Inouye Solar Telescope part 5: impacts of enhanced mirror and dichroic coatings on system polarization calibration. *J. Astron. Tel., Instr., Syst.*, 5:038001, July 2019.

[10] David M. Harrington, Sarah Jaeggli, Tom Schad, Amanda J. White, and Stacey R. Sueoka. Polarization modeling and predictions for Daniel K. Inouye Solar Telescope part 7: . *J. Astron. Tel., Instr., Syst.*, 7:in preparation, 2020.

[11] F. et al. Wöger. The DKIST Visible Broadband Imager. *Solar Phys.*, 296:(submitted), 2021.

[12] A. de Wijn and et al. The DKIST Visible Spectro-Polarimeter. *Solar Phys.*, 296:(in preparation), 2021.

[13] S. Jaeggli, et al. The DKIST DL-NIRSP. *Solar Phys.*, 296:(in preparation), 2021.

[14] A. Fehlmann and et al. The DKIST CRYO-NIRSP. *Solar Phys.*, 296:(in preparation), 2021.

[15] O. von der Lühe and et al. The DKIST VTF. *Solar Phys.*, 296:(in preparation), 2021.

[16] Friedrich Wöger. DKIST visible broadband imager interference filters. In *Proc. Soc. Photo-Opt. Instrum. Eng. (SPIE)*, volume CS-9147, page 91479I, August 2014.

[17] T. J. Kentischer, W. Schmidt, O. von der Lühe, M. Sigwarth, A. Bell, C. Halbgewachs, and A. Fischer. The visible tunable filtergraph for the ATST. In *Proc. Soc. Photo-Opt. Instrum. Eng. (SPIE)*, volume CS-8446, page 844677, September 2012.

[18] Wolfgang Schmidt, Matthias Schubert, Monika Ellwarth, Jörg Baumgartner, Alexander Bell, Andreas Fischer, Clemens Halbgewachs, Frank Heidecke, Thomas Kentischer, Oskar von der Lühe, Thomas Scheiffelen, and Michael Sigwarth. End-to-end simulations of the visible tunable filter for the Daniel K. Inouye Solar Telescope. In *Proc. Soc. Photo-Opt. Instrum. Eng. (SPIE)*, volume CS-9908, page 99084N, August 2016.

[19] Friedrich Wöger. Optical transfer functions derived from solar adaptive optics system data. *Appl. Opt.*, 49(10):1818–1825, April 2010.